SPECIAL ISSUE ARTICLE

The Anatomical Record WILEY
Advances in Integrative Anatomy and Evolutionary Biology

Morphological, osteological, and genetic data support a new species of *Madatyphlops* (Serpentes: Typhlopidae) endemic to Mayotte Island, Comoros Archipelago

Oliver Hawlitschek[1] [ID] | Mark D. Scherz[2] [ID] | Kathleen C. Webster[2] | Ivan Ineich[3] | Frank Glaw[2] [ID]

[1]Centrum für Naturkunde (CeNak), Universität Hamburg, Hamburg, Germany

[2]Zoologische Staatssammlung (ZSM-SNSB), Munich, Germany

[3]Institut de Systématique, Évolution, Biodiversité (ISYEB), Muséum National d'Histoire Naturelle, Sorbonne Université, École Pratique des Hautes Études, Université des Antilles, CNRS - CP, Paris, France

Correspondence
Oliver Hawlitschek, Centrum für Naturkunde (CeNak), Universität Hamburg, Martin-Luther-King-Platz 3, 20146 Hamburg, Germany.
Email: oliver.hawlitschek@gmx.de

Present address
Mark D. Scherz, Institute for Biochemistry and Biology, University of Potsdam, Karl-Liebknecht-Str. 24–25, 14476, Potsdam, Germany

Abstract

Blind snakes (Typhlopidae) are an enigmatic group of small burrowing snakes whose anatomy, phylogenetics, and biodiversity remain poorly known. *Madatyphlops comorensis* (Boulenger, 1889), endemic to the Comoros Archipelago in the Western Indian Ocean, is one of many species whose phylogenetic placement and generic assignment is unclear. We used DNA barcoding, external morphological examination, and osteological data from 3D reconstruction with micro-CT to study specimens of *Madatyphlops* from the Comoros Archipelago. Our results support the placement of *M. comorensis* in *Madatyphlops* and the recognition of the specimens from Mayotte Island as a closely related but distinct species, which we describe as *Madatyphlops eudelini* sp. nov. In this context, we present the first detailed osteological descriptions of any species of *Madatyphlops*, which we hope will serve as groundwork for further osteological studies in this genus and contribute to our limited but growing understanding of the osteology of typhlopid snakes.

KEYWORDS

3D reconstruction, blind snake, Comoros Archipelago, cranial anatomy, Mayotte, micro-CT, skull

1 | INTRODUCTION

Typhlopid snakes are among the squamates whose systematics and taxonomy remains most poorly studied (Miralles et al., 2018; Pyron & Wallach, 2014; Wallach, Williams, & Boundy, 2014; Wegener et al., 2013). Compared with many other snakes or lizards, the morphological study of typhlopids is more difficult due to their smaller size and possibly due to the adaptation of many anatomical characters to their cryptic, burrowing lifestyle. Probably owing to this lifestyle, many species are known from only very few specimens, most of which are historical museum specimens with poor or uncertain locality data.

In addition to a number of revisions on parts of the global diversity of typhlopid snakes (Graboski et al., 2019; Kornilios, 2017; Kornilios, Giokas, Lymberakis, & Sindaco, 2013), two recent comprehensive systematic revisions were published by Hedges, Marion, Lipp, Marin, and Vidal (2014) and Pyron and Wallach (2014).

These two works combined the study of external morphology with that of internal anatomy, osteology, and molecular genetics. The integrative approaches provided a much better resolution than any earlier study, and the genus *Typhlops*, which previously included the vast majority of all typhlopid snakes, was split into several genera (see also Miralles et al., 2018). However, even these comprehensive revisions leave many aspects of typhlopid systematics to be clarified and disagree on the placement of several taxa (Nagy et al., 2015).

One example of such disagreement is the species currently treated as *Madatyphlops comorensis* (Boulenger, 1889), endemic to the Comoros Archipelago in the Western Indian Ocean. Originally described as *Typhlops comorensis*, it was placed in *Afrotyphlops* by Hedges et al. (2014) and in *Madatyphlops* by Pyron and Wallach (2014). The latter placement was tentatively confirmed by Nagy et al. (2015), but additional data are required to resolve its classification and phylogenetic relationships reliably. Both generic assignments are plausible from a biogeographical point of view, as *M. comorensis* is restricted to the Comoros Archipelago situated halfway between Madagascar and continental Africa. The four volcanic islands of the Comoros Archipelago (Grand Comoro, Mohéli, Anjouan, and Mayotte) are typically assigned to the Malagasy faunal region (Louette, Meirte, & Jocqué, 2004) but also have Afrotropical faunal elements (Hawlitschek, Ramírez Garrido, & Glaw, 2017; Warren, Strasberg, Bruggemann, Prys-Jones, & Thébaud, 2010).

The type locality of the holotype (by monotypy) of *M. comorensis* ("Comoro Islands") was doubted by Meirte (2004) but later confirmed (Carretero, Harris, & Rocha, 2005; Hawlitschek, Brückmann, Berger, Green, & Glaw, 2011). Until recently, all known individuals of this species were found on Grand Comoro Island, with the exception of a single specimen found on Anjouan Island (Hawlitschek et al., 2011). Blanc (1971) erroneously cited this species from all four islands (see also de Massary et al., 2020). Apart from *M. comorensis* and an enigmatic typhlopid from Grand Comoro (Hawlitschek et al., 2011), the only other typhlopid snake known from the Comoros Archipelago so far is the introduced *Indotyphlops braminus* (Daudin, 1803), which is very common and widespread on all four major islands (Augros & Hawlitschek, 2019; Blanc, 1971; Hawlitschek et al., 2011).

During a field survey conducted on Mayotte Island in 2014, we discovered individuals of *Madatyphlops* resembling *M. comorensis* but also showing distinct differences to that species. Here, we provide a comparative study of their osteology, morphology, and genetics. According to their differences, we describe them here as a new species.

2 | MATERIALS AND METHODS

2.1 | Sampling

The two newly collected specimens from Mayotte Island representing different growth stages were fixed in 96% ethanol and subsequently stored in 70% ethanol. Tissue samples for molecular genetic analysis were stored in 96% ethanol. The sampling was conducted under research and export permits 82/DEAL/SEPR/2015 and ABSCH-IRCC-FR-247209-1. Specimens were deposited in the Zoologische Staatssammlung, Munich, Germany (ZSM). We also examined specimens of the Muséum National d'Histoire Naturelle, Paris, France (MNHN-RA) and the Natural History Museum, London (BMNH). A full list of the specimens included in the study is given in Table 1.

2.2 | Molecular genetics

We extracted DNA from tissue samples, amplified and sequenced the Cytochrome C Oxidase I (COI) marker as described in Hawlitschek, Nagy, Berger, and Glaw (2013). We then edited the sequence data in Geneious v.8.0.5 (Kearse et al., 2012), aligned the individual sequences using the Clustal function of MEGA X (Kumar, Stecher, Li, Knyaz, & Tamura, 2018), and reconstructed a Maximum Likelihood barcoding tree with 1,000 ultrafast bootstrap repeats in IQ-Tree (Hoang, Chernomor, von Haeseler, Minh, & Vinh, 2018; Trifinopoulos, Nguyen, von Haeseler, & Minh, 2016). We also used MrBayes 3.2.1 (Ronquist et al., 2012) with the GTR + G model, 30 million generations, and 10% burn-in to reconstruct a Bayesian barcoding tree. Finally, we calculated pairwise K2P distances in MEGA X. We uploaded the newly generated genetic data to GenBank under accession numbers MW497297 and MW497298.

2.3 | External morphology

We examined the external morphology of the two specimens collected on Mayotte Island, of eight specimens of *Madatyphlops* from Grand Comoro Island (ZSM 154/2010, 294/2018, MNHN-RA 1890.0027-0030, 1895.0126, 1902.0391), and of one from Anjouan (ZSM 164/2010), with the goal of detecting characters diagnostic of these lineages. We also took measurements of the *M. comorensis* holotype, BMNH 1946.1.11.92, whose island provenance is unknown. We took all measurements in mm with a digital caliper and took all scale counts with the aid of a stereo microscope. Following

TABLE 1 External morphological character states of *Madatyphlops* specimens examined

Island	Catalogue number	LOA	TL	MBD	MTW	MRW	HWE	TMD	LSR1	LSR2	LSR3	SC
Mayotte	ZSM 402/2014[a]	69.1	3.5	2.7	2.2	0.7	1.9	418	20	24	22	15
Mayotte	ZSM 403/2014[a]	190.7	6.9	4.0	3.2	1.2	3.0	414	20	24	22	15
Unknown	BMNH 1946.1.11.92	231.2[b]	3.2	3.7	3.3	0.8	2.3	403	–	22[c]	–	–
Anjouan	ZSM 164/2010	–	–	–	–	0.8	1.9	405	20	22	20	–
Grand Comoro	ZSM 154/2010	144.7[d]	–	2.8	–	0.9	1.9	372	18	22	18	–
Grand Comoro	ZSM 294/2018	213.9	4.8	3.3	2.5	1.1	2.7	445	20	22	22	10
Grand Comoro	MNHN-RA1902.0391	175.4	4.3.	3.7	2.6	0.9	1.8	429	–	22	–	11
Grand Comoro	MNHN-RA 1895.0126	207.6	4.4	3.5	3.0	0.7	2.5	424	–	22	–	11
Grand Comoro	MNHN-RA 1890.0027	211.0	4.6	3.7	2.6	1.0	2.3	388	22	22	20	15
Grand Comoro	MNHN-RA 1890.0028	179.0	3.3	2.4	1.7	0.8	2.2	430	22	22	20	14
Grand Comoro	MNHN-RA 1890.0029	102.0	2.0	1.7	1.4	0.9	1.9	395	22	22	20	17
Grand Comoro	MNHN-RA 1890.0030	108.0	2.5	1.8	1.3	0.7	1.8	406	22	22	20	13
Grand Comoro	Wallach and Glaw (2009)	117–245	–	3.0–4.5	–	–	–	414–485	–	22	–	12–15

Note: BMNH 1946.1.11.92 is the holotype of *M. comorensis*.

Abbreviations: HWE, head width at eye level; LOA, total length; LSR, number of longitudinal scale rows around first (1), second (midbody; 2), and third (3) third of body; SUC, number of subcaudal scales; MBD, midbody diameter; MRW, midrostral width; MTW, mean tail width; TAL, tail length; TMD, number of total middorsal scales.

[a] Assigned to the new species *Madatyphlops eudelini* sp. nov.

[b] 245 according to Boulenger (1889).

[c] 20 according to Boulenger (1889). Specimens listed under Wallach and Glaw (2009) provides a range of measurements taken from four individuals.

[d] Tail missing.

Pyron and Wallach (2014), we studied the following characters: LOA, total length; TAL, tail length; MBD, mid-body diameter; MTW, mean tail width; MRW, midrostral width; HWE, head width at eye level; TMD, number of total middorsal scales; LSR, number of longitudinal scale rows around first (1), second (2), and third (3) of body; SUC, number of subcaudal scales.

We then compared the measurements and scale counts among the island populations and to the range of measurements and counts provided of the specimens MNHN-RA 1889.0023-0026, 1895.0126, 1902.0391 from Grand Comoro in Wallach and Glaw (2009).

2.4 | Osteology

Osteological methods follow Chretien, Wang-Claypool, Glaw, and Scherz (2019). Micro-CT scans were produced using a phoenix|x nanotom m cone-beam scanner (GE Measurement & Control, Wunstorf, Germany). Scans were made using a tungsten target and a 0.1 mm Cu filter, at a current of 80 μA, voltage of 110 kV, timing of 750 ms, for 2,440 projections, for a total scan time of 30 min. Scans were reconstructed in datos|x reconstruct (GE Measurement & Control) and processed in VG Studio Max 2.2 (Volume Graphics GmbH, Heidelberg,
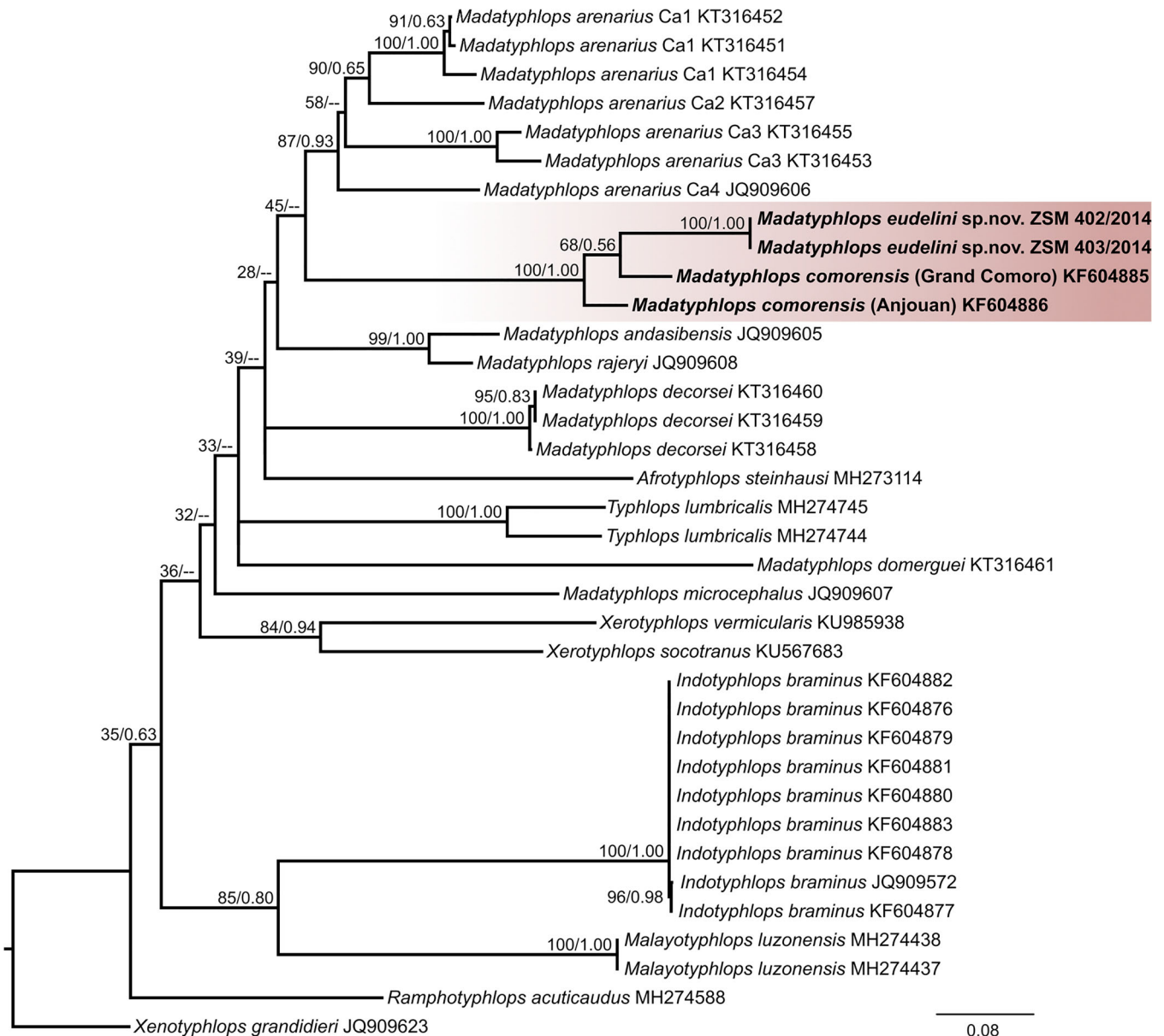

FIGURE 1 DNA barcoding tree based on COI sequence data of a sample of typhlopid snakes. The topology was reconstructed in IQtree and MrBayes, with bootstrap support/posterior probability given above nodes. *Madatyphlops* from the Comoros Archipelago form a clade (highlighted and bold). Nodes at genus or family levels are poorly resolved

TABLE 2   Genetic K2P distances of the COI gene measured in MEGA X

	M. eudelini sp. nov.	M. comorensis	M. andasibensis	M. arenarius	M. decorsei	M. domerguei	M. microcephalus	M. rajeryi	A. steinhausi	I. braminus	M. luzonensis	R. acuticaudatus	T. lumbricalis	X. socotranus	X. vermicularis	X. grandidieri
Madatyphlops eudelini sp. nov.	0.00															
Madatyphlops comorensis	0.10	0.08														
Madatyphlops andasibensis	0.18	0.19	n/c													
Madatyphlops arenarius	0.19	0.19	0.17	0.10												
Madatyphlops decorsei	0.21	0.21	0.17	0.17	0.00											
Madatyphlops domerguei	0.24	0.24	0.21	0.22	0.22	n/c										
Madatyphlops microcephalus	0.21	0.20	0.19	0.20	0.20	0.22	n/c									
Madatyphlops rajeryi	0.19	0.19	0.07	0.15	0.16	0.20	0.20	n/c								
Afrotyphlops steinhausi	0.19	0.19	0.19	0.18	0.20	0.21	0.20	0.20	n/c							
Indotyphlops braminus	0.23	0.22	0.21	0.21	0.22	0.24	0.21	0.19	0.22	0.00						
Malayotyphlops luzonensis	0.21	0.22	0.21	0.21	0.22	0.25	0.22	0.23	0.21	0.20	0.00					
Ramphotyphlops acuticaudatus	0.23	0.21	0.19	0.18	0.16	0.21	0.20	0.18	0.20	0.22	0.20	n/c				
Typhlops lumbricalis	0.23	0.22	0.20	0.18	0.20	0.23	0.20	0.19	0.20	0.22	0.23	0.21	0.10			
Xerotyphlops socotranus	0.21	0.20	0.17	0.19	0.18	0.21	0.20	0.17	0.21	0.21	0.20	0.19	0.20	n/c		
Xerotyphlops vermicularis	0.25	0.24	0.21	0.21	0.21	0.23	0.19	0.21	0.22	0.22	0.20	0.18	0.20	0.19	n/c	
Xerotyphlops grandidieri	0.21	0.21	0.19	0.17	0.19	0.23	0.21	0.19	0.19	0.23	0.19	0.18	0.18	0.22	0.21	n/c

Note: The matrix includes intraspecific and interspecific mean distances.
Abbreviation: n/c, not calculated.

Germany). Screenshots were produced using the Image Capture module. Due to a hard-drive failure, scans were lost and could not be deposited in a repository. The terminology of the skeletal elements mostly follows Chretien et al. (2019) and Cundall and Irish (2008).

2.5 | Taxonomic act

The electronic version of this article in Portable Document Format (PDF) will represent a published work according to the International Commission on Zoological Nomenclature (ICZN), and hence the new name contained in the electronic version is effectively published under that Code from the electronic edition alone. This published work and the nomenclatural act it contains have been registered in ZooBank, the online registration system for the ICZN. The ZooBank LSIDs (Life Science Identifiers) can be resolved and the associated information viewed through any standard web browser by appending the LSID to the prefix http://zoobank.org/. The LSID for this publication is urn:lsid:zoobank.org/:pub:7A79B48B-7333-4854-B185-A90C4BF33270. The online version of this work will be archived and made available from the following digital repositories: NCBI.

3 | RESULTS

3.1 | Molecular genetics

Our Bayesian and Maximum Likelihood DNA barcoding trees (Figure 1) retrieve the specimens from Mayotte in a highly supported (100 Bootstraps [BS]/1.00 Posterior Probability [PP]) cluster with the samples of *M. comorensis*. More specifically, *M. comorensis* from Anjouan is retrieved as sister to Mayotte + Grand Comoro, albeit with poor support (68 BS/0.56 PP). Overall, the bootstrap support and posterior probability of most nodes above the level of species is low, and many genera, such as *Madatyphlops*, are not retrieved as monophyletic in the barcoding tree. Our tree should be interpreted as indicating the degree of distinction between individuals but not as a robust phylogenetic hypothesis.

The COI sequences of the two specimens from Mayotte were found to be identical. The K2P distance to the *M. comorensis* specimen from Anjouan is 10.1%, and to the specimen from Grand Comoro 9.5%. The distance between the two *M. comorensis* specimens is 7.7%. The maximum intraspecific distances found are 14.8% in *M. arenarius*, 9.6% in *Typhlops lumbricalis*, 0.6% in *M. decorsei*, and 0.3% in *Indotyphlops braminus*.

Divergences between sibling species are 19.4% between *Xerotyphlops socotranus* and *X. vermicularis*, and 6.9% between *M. andasibensis* and *M. rajeryi*. A complete list of intra- and interspecific genetic distances is given in Table 2.

3.2 | Osteology

The following skull description of the new species described herein is based primarily on the adult specimen from Mayotte, ZSM 403/2014, with reference to the juvenile morphology of ZSM 402/2014, and in comparison to the skulls of two adult *Madatyphlops comorensis* (ZSM 154/2010 from Grand Comoro and ZSM 164/2010 from Anjouan), which are also presented here for the first time (Figure 2). Due to loss of the original scans (see above), the internal surfaces of the cranial bones could not be studied. Throughout this description, we anticipate our formal taxonomic conclusions and refer to the animals from Mayotte as *Madatyphlops eudelini* sp. nov. (described below).

Snout complex: The skulls of both *Madatyphlops* species are typical of typhlopids (Cundall & Irish, 2008; List, 1966; Tihen, 1945). The snout is bulbous, as wide as the parietals, and the frontals narrow, with their midpoint narrower than the lateral extent of the nasals. The snout is composed of the premaxilla, septomaxillae (paired), vomers (paired), nasals (paired), and prefrontals (paired). The external naris is large and oblong, bordered by the prefrontal laterally, nasal anteriorly, premaxilla medially, with posteriorly a small amount of participation by anterolateral flanges of the septomaxilla.

The premaxilla forms the anterior base of the snout. It is edentulous, composed of a vertical anterior plate with an angled edge between the nasals, a horizontal *pars palatina* with posteriorly oriented lateral flanges, and an elongated vomerine process, which dorsally bears a medial septum. It is in contact with the nasals anterodorsally, the septomaxillae posterolaterally, and interdigitates between the vomers via its elongated vomerine process. It is pierced by several foramina, receiving the *ophthalmicus profundus* of the trigeminal (Haas, 1964). A pair of these foramina are oriented anteriorly at the anterior lip of the premaxilla, and a second pair ventrally, as well as a concavity and tube formed along the midline at the base of the vomerine process.

The nasal is a broad, roughly lenticular element. It articulates with the frontal posteriorly, prefrontal laterally, premaxilla anteriorly, and its contralateral medially. The receiving surface for the frontal is an elongated shelf, suggesting some degree of kinesis. A circular foramen is
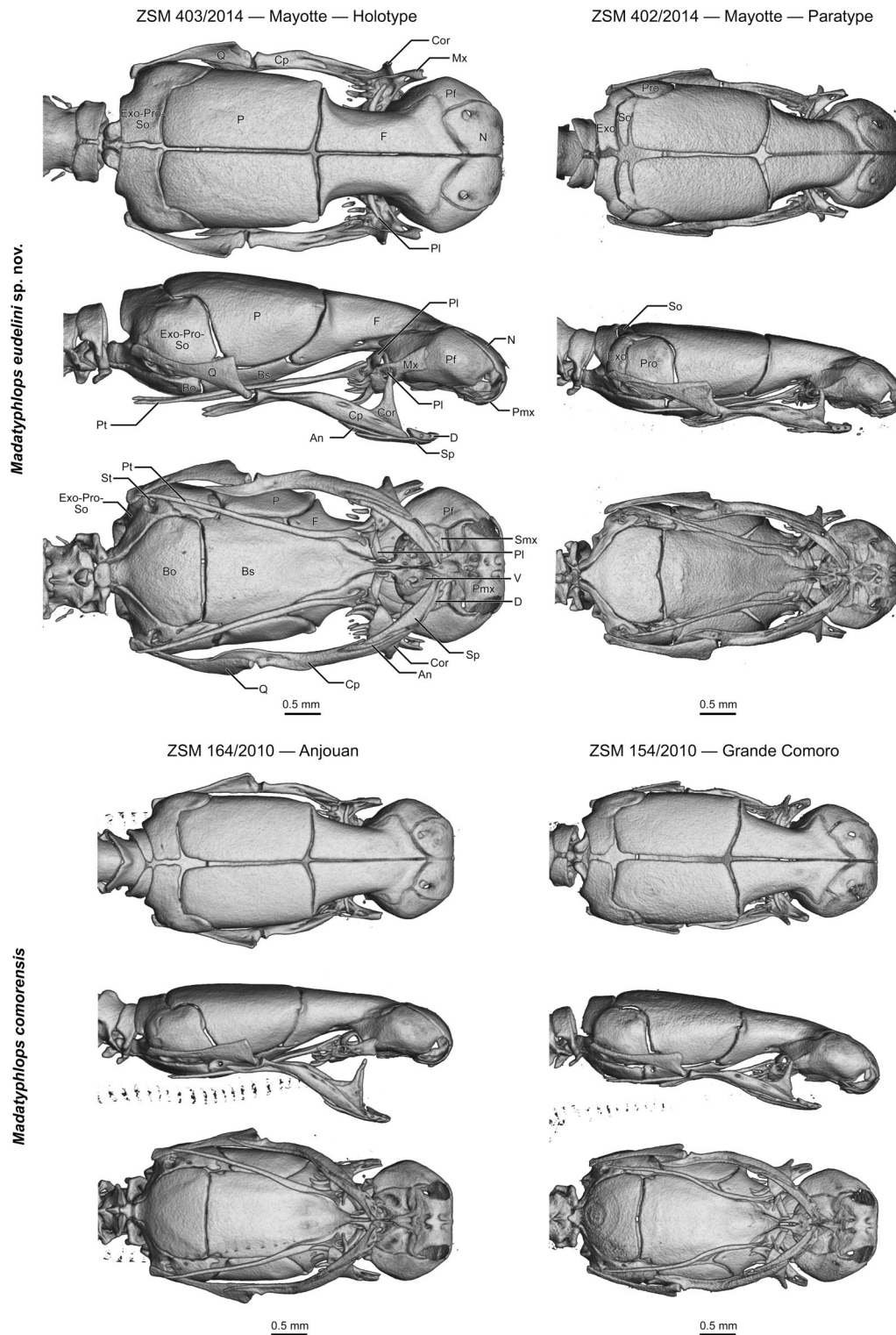
FIGURE 2 Micro-computed tomography reconstructions of the skulls of *Madatyphlops eudelini* sp. nov. and *M. comorensis*. Abbreviations: An, angular; Bo, basioccipital; Bs, basisphenoid; Cor, coronoid; Cp, compound; D, dentary; Exo, exoccipital; F, frontal; Mx, maxilla; N, nasal; P, parietal; Pf, prefrontal; Pl, palatine; Pmx, premaxilla; Pro, prootic; Pt, pterygoid; Q, quadrate; Smx, septomaxilla; So, supraoccipital; Sp, splenial; St, stapes; V, vomer

present towards the prefrontal-frontal corner (typical of typhlopids; Evans, 1955; List, 1966; Rieppel, Kley, & Maisano, 2009).

The prefrontal is a convex element that constitutes the lateral wall of the snout complex. It articulates with the nasal anterodorsomedially, frontal posterodorsomedially

to posteriorly, and septomaxilla ventromedially. It is excluded from contact with the prevomer ventrally by the anterolateral flange of the septomaxilla. The prefrontal's lateral outline in dorsal view is more angular in the more mature *M. eudelini* sp. nov. holotype compared to its rather rounded outline in the paratype. In this respect, the specimens of *M. comorensis* are also more like the adult holotype of *M. eudelini* sp. nov. than the juvenile of similar skull size. The posterior-most extent of the prefrontal is well separated from the optic foramen of the frontal, as stated by Chretien et al. (2019).

The septomaxilla articulates with the vomer posteromedially, the vomerine process of the premaxilla medially, the lateral flanges of the premaxilla anteriorly, and the prefrontal laterally. It might also have posterior contact with the frontal and/or basisphenoid, but this cannot be established based on our available data. The participation of this bone in the external naris is achieved by a narrow lateral flange. A pronounced mediolateral furrow is present in the ventral surface of the bone at roughly half the length of the vomerine process of the premaxilla. In *M. eudelini* sp. nov., this furrow is straight and slightly posteriorly oriented, whereas in *M. comorensis*, it is somewhat curved.

The vomer sits between the septomaxillae along the midline. As is typical of typhlopoids (Chretien et al., 2019; List, 1966), it bears an extended posterior process that forms the medial articulating surface for the palatine's medial ramus as part of the rotational jaw mechanism. Laterally, it has a pronounced *fenestra vomeronasalis* that is not closed along its lateral edge. The ventral surface bears two foramina, one oriented anteriorly, the other ventrally.

Upper jaw mechanism: The upper jaw mechanism is much like that of other typhlopoids, as has been described in some detail by Iordansky (1997), Cundall and Irish (2008), and Chretien et al. (2019), and is discussed by Strong et al. (n.d., this volume); our discussion of it here is therefore only brief: the long, thin, y-shaped pterygoid articulates with the pterygoid ramus of the roughly μ-shaped palatine, the medial ramus of which articulates with the posterior process of the vomer, while its lateral ramus passes through the palatine foramen of the maxilla, which is a small, roughly rectangular element with curved teeth along its ventral margin. This gives the ability for the maxilla to rotate around the middle axis of the bone while simultaneously swinging forward to engage in maxillary raking (Kley, 2001). The structures of these bones do not differ overtly between *M. comorensis* and *M. eudelini* sp. nov.

It is worth mentioning that the anterior surface of the dorsal end of the maxilla has a deep groove into which the keyhole fenestra of Chretien et al. (2019) opens. It is

more pronounced than in the Malagasy genus *Xenotyphlops*, but its function is not known. Additionally, the number and degree of development of teeth is worthy of comment: in the holotype of the new species, the anterior three teeth are fully mineralized, and there are six additional teeth behind them that vary in development. In the paratype, there is only one fully developed tooth, but several additional developing teeth are present behind it. In our specimens of *M. comorensis*, there are one or two fully mineralized teeth and roughly four to five developing teeth behind them.

Cranium: The cranium is composed of the frontals (paired), parietals (paired), basisphenoid, basioccipital, and a pair of fused elements comprised of the exoccipital, prootic, and supraoccipital. Even in the large holotype of *M. eudelini* sp. nov., there are substantial gaps between most of these bones, suggesting substantial cranial kinesis. The exoccipital-prootic-supraoccipital element is strongly fused in the adult *M. eudelini* sp. nov., but in juveniles, this element is evidently not yet fused (Figure 2). Whilst still unfused, the supraoccipitals are paired. In contrast, individuals of *M. comorensis* of similar skull size to our juvenile *M. eudelini* sp. nov. specimen have these elements strongly fused.

The frontal is a bowed bone comprising the anterolateral brace of the brain case. Its dorsal surface is flat and its lateral surface curved. The mid-extent of the frontal is something of a bottleneck in the skull, and it flares at either end, posteriorly to the parietal, anteriorly to the snout complex. The lateral outline of the mid-section is most parallel in the holotype of *M. eudelini* sp. nov. but slopes obliquely inward anteriorly in the paratype and in *M. comorensis*. The frontal is in contact with the parietal posteriorly along a long, dorsally straight and ventrally posteriorly curving margin, the basisphenoid ventrally along an oblique margin, prefrontal anterolaterally, and nasal anteromedially, as well as its contralateral dorsomedially. It may also contact the septomaxilla anteroventromedially, but this is not possible to assess from the available data. The oblong optic foramen sits in a groove posterior to the end of the prefrontal. A diminutive foramen at the posteroventral corner of the frontal probably transmits the maxillary branch of the trigeminal nerve (Chretien et al., 2019). In the paratype of *M. eudelini* sp. nov., the posterodorsal margin of the frontal is obliquely slanted. Presumably, this becomes more straightened and exaggerated with age.

The parietal is a convexly curved bone. Its dorsal surface is mostly flat, but curves gently laterally (as opposed to the rather stark border of dorsal and lateral in the frontal). The ventrolateral edge is smoothly curved. It is in contact with the frontal anteriorly, basisphenoid

ventrally, and the fused exoccipital-prootic-supraoccipital element posteriorly, as well as its contralateral dorsomedially. The posterior edge of the bone is somewhat sigmoid curved, extending dorsally beyond its ventral extent. In the holotype of *M. eudelini* sp. nov., a distinct tuberosity is formed at the brace of the posterodorsolateral point of the frontal. This appears to be ontogenetic and is weakly expressed in the smaller paratype of *M. eudelini* sp. nov. In *M. comorensis*, these tuberosities are also developed.

The paired exoccipital-prootic-supraoccipital element composes the entire posterodorsal portion of the skull, forming the lateral elements of the occipital condyle. As mentioned above, fusion apparently progresses during maturation/growth. The prootic portion of the bone is a rotund element in the posterolateral corner of the cranium. The exoccipital portion comprises the posterior element, including the lateral occipital condyle and dorsal arch, and the supraoccipital comprises the anterior dorsal arch and occludes the exoccipital from contact with the parietal. The element is in contact with the parietal anteriorly, basioccipital ventrally, and basisphenoid through a small contact anteroventrally (not to mention the first vertebra), as well as the contralateral medially both dorsally and ventrally. Additionally, it has a lateral articular surface with the quadrate, lying behind the *fenestra ovalis*. The *fenestra ovalis* is small, almost wholly filled by the stapes. The *recessus scalae tympani* is slightly smaller than the *fenestra ovalis*, oriented anteroventrally, situated directly below the *fenestra ovalis*. The trigeminal foramen is only posteriorly bordered by this element; its anterior border is made up by the parietal. The carotid channel is only partly covered.

The stapes sits deep inside the *fenestra ovalis* of the exoccipital-prootic-supraoccipital and is only visible by its short stylus.

The basioccipital is a single, largely triangular element, forming the ventral component of the occipital condyle and posteroventral part of the braincase. It is in contact dorsolaterally with the exoccipital-prootic-supraoccipital and anteriorly with the basisphenoid. Note that the circular patterns evident in ZSM 154/2010 in this bone are certainly scanning artifacts.

The basisphenoid is a single, large, triangular element comprising most of the ventral surface of the braincase. It is in contact with the basioccipital posteriorly, the exoccipital-prootic-supraoccipital briefly posterolaterally, the parietal laterally, and the frontal anterolaterally. It probably extends also between the septomaxillae, but this is not clear from our data. At the posterolateral corners, this bone is penetrated by the vidian canal. This canal is much more visible in *M. comorensis* than in *M. eudelini* sp. nov., forming concavities below the canal entry.

Suspensorium and mandible: The suspensorium and mandible is composed of the quadrate, compound, angular, splenial, coronoid, and dentary. It is typical of typhlopids (see Strong et al. n.d., this volume).

The quadrate is a roughly triangular bone, with its cephalic process in the anterior half of the bone, and a long otic process that articulates posteriorly with the lateral surface of the exoccipital-prootic-supraoccipital element. Its mandibular process is received by the articulation of the compound.

The compound is longer than the quadrate. It articulates posteriorly with the quadrate, anteroventrally with the angular and splenial, anterodorsally with the coronoid and anteriorly approaches but does not contact the dentary. It has an elongated retroarticular process behind the articulation with the quadrate. Its lateral surface is pierced by anterior and posterior surangular foramina. Around midway along its length, the dorsal surface is pierced by the Meckelian canal. Anteriorly its ventral surface is concave to receive the angular.

The angular is a simple, narrow sliver of bone bracing the ventral Meckelian canal between the coronoid, splenial, and compound. The coronoid is a triangular bone with an elongated dorsal extension. It is ventrally in contact with the compound posteriorly and splenial anteriorly. The splenial is a curved, sculpted bone, comprising the ventral anterior portion of the jaw, and guiding the Meckelian canal. Posterodorsally, it is in contact with the angular, the compound, more medially with the coronoid, and anterodorsally with the dentary. Finally, the dentary is a short element with numerous mental foramina along its anterior surface, apparently in sole contact with the splenial, ventrally. The two lower jaws are rather widely separated medially from one another.

In summary, the osteology of *M. eudelini* sp. nov., formally described as a new species below, is highly similar to that of *M. comorensis*. The main differences appear to be the shape of the mediolateral groove in the ventral septomaxilla (straight in *M. eudelini* sp. nov., curved in *M. comorensis*) and the concavities ventral to the vidian canal (present in *M. comorensis* vs. absent or weak in *M. eudelini* sp. nov.).

3.3 | Taxonomic act

3.3.1 | Genus *Madatyphlops* Hedges et al., 2014

Madatyphlops eudelini *sp. nov.*
LSID for this species: urn:lsid:zoobank.org/: pub:7A79B48B-7,333-4,854-B185-A90C4BF33270.
Available names: None.

FIGURE 3 The holotype (ZSM 403/2014) of *Madatyphlops eudelini* sp. nov. (a) Specimen found freshly dead at the type locality. (b) Close-up lateral view of the head and anterior body. (c) The specimen preserved in ethanol, lateral view of the whole specimen. (d) Head and neck, dorsal view. (e) Head and neck, lateral view. (f) Head and throat, ventral view. Photos (a) and (b) by Rémy Eudeline, (c) by Oliver Hawlitschek, (d) to (f) by Michael Franzen

Holotype: ZSM 403/2014 (FGZC 4983; Figure 3), adult, sex undetermined, collected when apparently freshly dead on October 15, 2014, at 12.88177°S, 45.16921°E, 585 m a.s.l., on a trail in primary humid forest on the ascent of Mt. Benara from Bandrele, Mayotte (a French oversea department, Comoros Archipelago), by R. Eudeline.

Paratype: ZSM 402/2014 (FGZC 4981), juvenile, sex undetermined, collected while active in the leaf litter on November 14, 2014, same locality as holotype, by O. Hawlitschek, M.D. Scherz, C.Y.H. Wang-Claypool, L. Montfort, and R. Eudeline.

Etymology: The species epithet is a patronym in honor of Rémy Eudeline, with the last letter removed for

better pronunciation. Rémy is a high school teacher of sciences, parataxonomist, and then-resident of Mayotte, who found the holotype specimen during his first visit to the type locality, after the first author of this publication failed to observe this species in more than 10 surveys of the same locality.

Diagnosis: *Madatyphlops eudelini* sp. nov. is diagnosed by the following combination of characters: Maximum known total length 190.7 mm; dorsal coloration dark with a cream-white band of the width of two scale rows along the mid-venter; scales around midbody 24; total middorsal scales 414–418; subcaudal scales 15. Assigned to the genus *Madatyphlops* based on molecular genetic data, that is, placement as sibling taxon of *M. comorensis* nested within the clade of *Madatyphlops*, and on the agreement of the morphological characters studied (Table 1) with the diagnosis of *Madatyphlops* given in Hedges et al. (2014), and Pyron and Wallach (2014). The following diagnosis is based on previously published comparative data (Renoult & Raselimanana, 2009; Wallach & Glaw, 2009; Wegener et al., 2013) and data collected for this study (Table 1). *Madatyphlops eudelini* sp. nov. differs from all other Comoran and most Malagasy species of blindsnakes (except several specimens of the *M. microcephalus* complex) by its dark dorsal coloration combined with a cream-white band of the width of two scale rows along the mid-venter, broader under chin and tail. It further differs from the syntopic *Indotyphlops braminus* by more scales around midbody (24 vs. 20), larger maximum total length (up to 191 mm vs. up to ca. 180 mm); and from the Malagasy *Xenotyphlops grandidieri* by more scales around midbody (24 vs. 20–22), dorsal coloration (black vs. pink), and head morphology (visible eyes vs. no eyes, lack of enlarged head plate, and skull morphology; Chretien et al., 2019). It differs from the other *Madatyphlops* species as follows: by more scales around midbody (24) from *M. ocularis* (20), *M. microcephalus* (20), *M. reuteri* (20), *M. boettgeri* (20–21), *M. comorensis* (22), *M. domerguei* (22), and several populations of the *M. arenarius* complex (20); and by fewer scales around midbody (24) from *M. andasibensis* (26), *M. decorsei* (26–28), and some populations of *M. mucronatus* (24–28). *Madatyphlops eudelini* sp. nov. differs from *M. rajeryi* by dorsal coloration (black vs. yellowish-gray), smaller maximum total length (191 vs. 272 mm), and smaller midbody diameter (2.7–4.0 vs. 7.4 mm); from *M. madagascariensis* by a lower number of total middorsal scales (414–418 vs. 580), smaller maximum total length (191 vs. 410 mm), and the presence of distinct eyes (vs. invisible); from *M. arenarius* by dorsal coloration (black vs. pink), eye coloration (pale vs. black); and from *M. mucronatus* by a lower number of total middorsal scales (414–418

vs. 488–577), smaller maximum total length (191 vs. 418 mm), and smaller midbody diameter (2.7–4.0 vs. 3.0–8.5 mm). It differs from *M. albanalis* by smaller maximum total length (up to 191 mm vs. 270 mm), more scales around midbody (24 vs. 20), and rostral not protruding vs. strongly protruding. The geographical origin of *M. albanalis* and its assignment to *Madatyphlops* are dubious (Wallach et al., 2014). The attribution of *M. cariei*, which is known only from seven subfossil trunk vertebrae from Mauritius, is unclear, and we are unable to provide any diagnosis with the available data (Wallach et al., 2014).

There are no osteological descriptions of any other *Madatyphlops* species available. Therefore, we can compare the skull of the new species only to that of *M. comorensis*. From that species, it differs only subtly in the shape of the groove in the septomaxilla and in the concavities of the vidian canal in the basisphenoid (see above). The skulls of these snakes are highly conserved but show substantial ontogenetic shape change.

Description of the holotype: ZSM 403/2014 overall well preserved, external damage in lateral body from tissue sampling for molecular genetic analysis visible.

Total length 190.7 mm, tail length 6.9 mm, midbody diameter 4.0 mm, mean tail width 3.2 mm, midrostral width 1.2 mm, and head width at eye level 3.0 mm. Number of total middorsal scales 414. Number of longitudinal scale rows around first third of body 20, around second third of body (at midbody) 24, around third third of body 22. Number of subcaudal scales 15.

Head round, slightly wider than neck before tapering towards the snout. Snout depressed, rounded in lateral aspect. Nostrils round, closer to rostral than to preocular. Inferior nasal suture in contact with first and second supralabial, nasal with strongly concave posterior border. Preocular single, about as wide as nasal. Ocular slightly wider than preocular. Eye round with visible pupil, located under ocular adjacent to preocular. Postoculars two, parietals two, supralabials four.

Color in preservative dorsally and laterally overall dark brown. Scales transparent. Venter with cream-white medial band of the width of two scale rows, broadening under head and tail.

Variation: The morphology of the paratype ZSM 402/2014 largely agrees with that of the holotype, except in its much smaller size. This size difference has clear consequences also for the osteological differences between the two specimens. Both specimens agree in the specific ventral colorations. Measurements and counts are given in Table 1.

Distribution, natural history, and conservation: Our analyses retrieve *Madatyphlops eudelini* sp. nov. as the closest relative of *M. comorensis*, which is endemic to the

neighboring islands of the Comoros Archipelago, suggesting that *M. eudelini* sp. nov. is endemic to Mayotte. It is known only from two specimens from one high-elevation locality, which indicates an extremely limited geographic range (unlikely to be more than 20 km^2; Figure 4). Despite intensive searches, the new species has never been found at lower elevation, where most habitats are degraded. This suggests that it may be dependent on natural forest habitats, which originally covered most of Mayotte (Paris, 1999). The introduced, parthenogenetic *I. braminus* is common in degraded lowland habitats and is slightly smaller, but we cannot exclude competition with the native species, which may pose an additional threat and further restrict *M. eudelini* sp. nov. to the remaining natural upland habitats. These remaining natural forests of Mayotte are legally protected and currently stable, but future changes in land use and increasing urbanization may lead to severe declines in the quality and extent of the remaining habitat, which may rapidly drive the species to an extremely high risk of extinction. Therefore, we suggest that *M. eudelini* sp. nov. may qualify for the state of Vulnerable under the IUCN Red List criterion VU D2.

4 | DISCUSSION

The new typhlopid snake here described as *Madatyphlops eudelini* sp. nov. is clearly distinct from all other typhlopids of the region. Morphological and osteological data support its placement in the genus *Madatyphlops* and diagnose it from all congeneric species and from the sympatric *Indotyphlops braminus*. Genetic data further support this distinction. In a DNA barcoding project of reptiles from Madagascar, Nagy, Sonet, Glaw, and Vences (2012) found the average K2P distance of COI
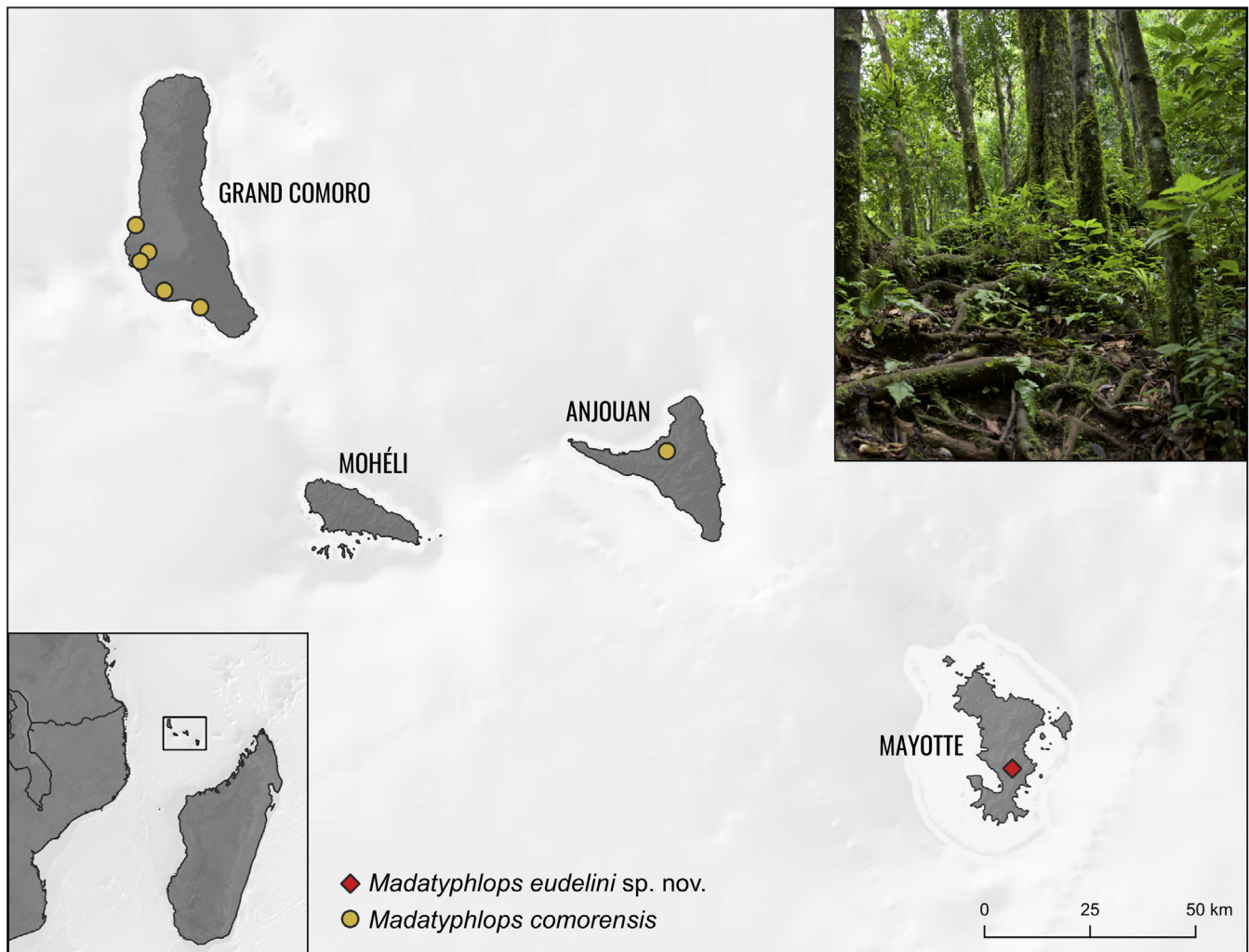

FIGURE 4 Distribution map of *Madatyphlops* in the Comoros Archipelago. The inlays show the position of the archipelago in the context of the Western Indian Ocean (bottom left) and a photo of the type locality of *Madatyphlops eudelini* sp. nov., the humid forest of Mt. Benara on Mayotte Island (top right)

between any two typhlopid species to be 18.6% and between the sister pair of *M. andasibensis* and *M. rajeryi* 6.9%, in agreement with our own results. With 9.5% and 10.1%, the distances found between *M. eudelini* sp. nov. and *Madatyphlops* from Grand Comoro and Anjouan surpass the value found between *M. andasibensis* and *M. rajeryi*. With a K2P distance of 7.7%, the *Madatyphlops* specimen from Anjouan is genetically very distinct from the specimen from Grand Comoro. However, we did not find any diagnostic morphological or osteological differences. Since only a single damaged specimen from Anjouan was available to us, we were not able to study all characters of known diagnostic value in *Madatyphlops*. We suggest that the *Madatyphlops* specimen from Anjouan may represent another distinct lineage whose taxonomic status can only be clarified after more data become available.

According to our DNA barcoding tree, *Madatyphlops* from the Comoros Archipelago form a well-supported clade. The relationships within this clade are not clearly resolved. The tree also fails to resolve any higher-level relationships, but it supports the view of a single origin of all Comoran *Madatyphlops*. After describing *M. eudelini* sp. nov., the monophyly of *M. comorensis* (i.e., *Madatyphlops* from Grand Comoro and Anjouan) is not supported. We refrain from drawing any further phylogenetic or taxonomic conclusions from this tree because it is based on a single mitochondrial marker, which may produce misleading results especially at a deeper phylogenetic level. More extensive genetic sampling will be required to resolve the phylogenetic relationships and biogeographic history of the typhlopid snakes of this Indian Ocean archipelago.

Most native reptile species of the Comoros Archipelago belong to lineages of Malagasy origin, many of which have colonized all four islands of the archipelago and formed endemic clades (Hawlitschek, Ramírez Garrido, & Glaw, 2017). The assignment of all native typhlopid species to the otherwise Malagasy genus *Madatyphlops* largely follows this pattern, except the island of Mohéli, from which no native typhlopid snake has so far been reported, despite dedicated searches in surveys for this and for earlier projects (Hawlitschek et al., 2017; Hawlitschek & Glaw, 2013; Hawlitschek, Nagy, & Glaw, 2012; Hawlitschek, Scherz, Straube, & Glaw, 2016). Nevertheless, we suspect that *Madatyphlops* has also colonized Mohéli, and the native lineage remains to be found.

In addition to *M. comorensis* and *I. braminus*, there exist two specimens of a third typhlopid snake species captured on Grand Comoro in 2000 (Hawlitschek et al., 2011). Preliminary genetic and morphological analyses (unpublished data by O. Hawlitschek) have shown that these specimens are different from, and probably not closely related to, all other typhlopid snakes known from the Comoros Archipelago, which means that their identity remains unclear. Unlike *M. comorensis* and *M. eudelini* sp. nov., these specimens were found in lowland environments near the capital town of Moroni. Despite dedicated efforts at the same and other localities, no specimens were detected after 2000. Possibly, this species is not native to Grand Comoro, but represents an unknown introduced species, as reflected by its apparent urban distribution near the island's main port.

Osteologically, the new species *M. eudelini* sp. nov. is highly conservative, showing strong similarities to *M. comorensis*, the only other member of the genus that has been examined in detail. These species are very similar to the only other *Madatyphlops* studied osteologically so far, *Madatyphlops boettgeri*, which was investigated by List (1966; as *Typhlops boettgeri*) alongside numerous other typhlopids. The only substantial difference between that species and those studied here is its lack of fusion of the prootic with the exoccipital and supraoccipital, although the extent of some bones, such as the frontals, does seem to differ as well. The detailed description provided here will hopefully serve as the groundwork for understanding the apparent conservative skull morphology and systematics of the entire *Madatyphlops* genus, and place them within our growing but still limited understanding of the skull diversity of Typhlopoidea as a whole.

AUTHOR CONTRIBUTIONS

Oliver Hawlitschek: Conceptualization; data curation; formal analysis; funding acquisition; investigation;

methodology; project administration; resources; software; supervision; validation; visualization; writing-original draft; writing-review and editing. **Mark Scherz:** Conceptualization; data curation; formal analysis; investigation; methodology; software; supervision; validation; visualization; writing-review and editing. **Kathleen Webster:** Data curation; formal analysis; investigation; methodology; software; visualization; writing-review and editing. **Ivan Ineich:** Formal analysis; resources; validation; writing-review and editing. **Frank Glaw:** Conceptualization; resources; supervision; validation; writing-review and editing.

CONFLICT OF INTEREST
The authors declare no conflicts of interest.

ETHICS STATEMENT
No experiments on living animals were conducted. The sampling was conducted under research and export permit 82/DEAL/SEPR/2015 and ABSCH-IRCC-FR-247209-1.

DATA AVAILABILITY STATEMENT
All genetic data will be made available on GenBank upon manuscript acceptance.

ORCID
Oliver Hawlitschek https://orcid.org/0000-0001-8010-4157
Mark D. Scherz https://orcid.org/0000-0002-4613-7761
Frank Glaw https://orcid.org/0000-0003-4072-8111

REFERENCES
Augros, S., & Hawlitschek, O. (2019). Monographies. In S. Augros (Ed.), *Atlas des Reptiles et Amphibiens Terrestres de l'archipel des Comores. Paris: Biotope éditions, Mèze, MNHN* (pp. 81–213). Paris: Biotope éditions, Mèze, MNHN.
Blanc, C. P. (1971). Les Reptiles de Madagascar et des îles voisines. *Annales Université Madagascar (Sciences)*, *8*, 95–178.
Boulenger, G. A. (1889). Descriptions of new Typhlopidæ in the British Museum. *Annals and Magazine of Natural History*, *6*, 360–363.
Carretero, M. A., Harris, D. J., & Rocha, S. (2005). Recent observations of reptiles in the Comoro islands (Western Indian Ocean). *The Herpetological Bulletin*, *91*, 19–28.
Chretien, J., Wang-Claypool, C. Y., Glaw, F., & Scherz, M. D. (2019). The bizarre skull of *Xenotyphlops* sheds light on synapomorphies of Typhlopoidea. *Journal of Anatomy*, *234*, 637–655.
Cundall, D., & Irish, F. J. (2008). The snake skull. In C. Gans, A. S. Gaunt, & K. Adler (Eds.), *The skull of Lepidosauria* (pp. 349–692). Society for the Study of Amphibians and Reptiles: Ithaca, New York.
Daudin, F. M. (1803). *Histoire Naturelle, Générale et Particulière des Reptiles* (Vol. 7, p. 436). Paris: Dufart.

de Massary, J. C., Bour, R., Dewynter, M., Frétey, T., Glaw, F., Hawlitschek, O., … Lescure, J. (2020). Liste taxinomique de l'herpétofaune dans l'outre-mer français: IV. Département de Mayotte. *Bulletin de la Société Herpétologique de France*, *173*, 9–26.
Evans, H. E. (1955). The osteology of a worm snake, *Typhlops jamaicensis* (Shaw). *The Anatomical Record*, *122*, 381–396.
Graboski, R., Arredondo, J. C., Grazziotin, F. G., da Silva, A. A. A., Prudente, A. L. C., Rodrigues, M. T., … Zaher, H. (2019). Molecular phylogeny and hemipenial diversity of South American species of *Amerotyphlops* (Typhlopidae, Scolecophidia). *Zoologica Scripta*, *48*, 139–156.
Haas, G. (1964). Anatomical observations on the head of *Liotyphlops albirostris* (Typhlopidae, Ophidia). *Acta Zoologica*, *45*, 1–62.
Hawlitschek, O., & Glaw, F. (2013). The complex colonization history of nocturnal geckos (*Paroedura*) in the Comoros Archipelago. *Zoologica Scripta*, *42*, 135–150.
Hawlitschek, O., Brückmann, B., Berger, J., Green, K., & Glaw, F. (2011). Integrating field surveys and remote sensing data to study distribution, habitat use and conservation status of the herpetofauna of the Comoro Islands. *Zookeys*, *144*, 21–78.
Hawlitschek, O., Nagy, Z. T., & Glaw, F. (2012). Island evolution and systematic revision of Comoran snakes: Why and when subspecies still make sense. *PLoS One*, *7*, e42970.
Hawlitschek, O., Nagy, Z. T., Berger, J., & Glaw, F. (2013). Reliable DNA barcoding performance proved for species and island populations of Comoran squamate reptiles. *PLoS One*, *8*, e73368.
Hawlitschek, O., Scherz, M. D., Straube, N., & Glaw, F. (2016). Resurrection of the Comoran fish scale gecko *Geckolepis humbloti* Vaillant, 1887 reveals a disjunct distribution caused by natural overseas dispersal. *Organisms, Diversity and Evolution*, *16*, 289–298.
Hawlitschek, O., Ramírez Garrido, S., & Glaw, F. (2017). How marine currents influenced the widespread natural overseas dispersal of reptiles in the Western Indian Ocean region. *Journal of Biogeography*, *44*, 1435–1440.
Hawlitschek, O., Toussaint, E. F. A., Gehring, P. S., Ratsoavina, F. M., Cole, N., Crottini, A., … Glaw, F. (2017). Gecko phylogeography in the Western Indian Ocean region: The oldest clade of *Ebenavia inunguis* lives on the youngest Island. *Journal of Biogeography*, *44*, 409–420.
Hedges, S. B., Marion, A. B., Lipp, K. M., Marin, J., & Vidal, N. (2014). A taxonomic framework for typhlopid snakes from the Caribbean and other regions (Reptilia, Squamata). *Caribbean Herpetology*, *49*, 1–61.
Hoang, D. T., Chernomor, O., von Haeseler, A., Minh, B. Q., & Vinh, L. S. (2018). UFBoot2: Improving the ultrafast bootstrap approximation. *Molecular Biology and Evolution*, *35*, 518–522.
Iordansky, N. N. (1997). Jaw apparatus and feeding mechanics of *Typhlops* (Ophidia: Typhlopidae): A reconsideration. *Russian Journal of Herpetology*, *4*, 120–127.
Kearse, M., Moir, R., Wilson, A., Stones-Havas, S., Cheung, M., Sturrock, S., … Drummond, A. (2012). Geneious basic: An integrated and extendable desktop software platform for the organization and analysis of sequence data. *Bioinformatics*, *28*, 1647–1649.
Kley, N. J. (2001). Prey transport mechanisms in blindsnakes and the evolution of unilateral feeding systems in snakes. *American Zoologist*, *41*, 1321–1337.

Kornilios, P. (2017). Polytomies, signal and noise: Revisiting the mitochondrial phylogeny and phylogeography of the Eurasian blindsnake species complex (Typhlopidae, Squamata). *Zoologica Scripta*, *46*, 665–674.

Kornilios, P., Giokas, S., Lymberakis, P., & Sindaco, R. (2013). Phylogenetic position, origin and biogeography of Palearctic and Socotran blind-snakes (Serpentes: Typhlopidae). *Molecular Phylogenetics and Evolution*, *68*, 35–41.

Kumar, S., Stecher, G., Li, M., Knyaz, C., & Tamura, K. (2018). MEGA X: Molecular evolutionary genetics analysis across computing platforms. *Molecular Biology and Evolution*, *35*, 1547–1549.

List, J. C. (1966). Comparative osteology of the snake families Typhlopidae and Leptotyphlopidae. *Illinois Biological Monographs*, *36*, 1–112.

Louette, M., Meirte, D., & Jocqué, R. (2004). *La faune terrestre de l'archipel des Comores*. Tervuren: MRAC.

Meirte, D. (2004). Reptiles. In M. Louette, D. Meirte, & R. Jocque (Eds.), *La Faune Terrestre de l'archipel des Comores* (pp. 201–224). Tervuren: MRAC.

Miralles, A., Marin, J., Markus, D., Herrel, A., Hedges, S. B., & Vidal, N. (2018). Molecular evidence for the paraphyly of Scolecophidia and its evolutionary implications. *Journal of Evolutionary Biology*, *31*, 1782–1793.

Nagy, Z. T., Sonet, G., Glaw, F., & Vences, M. (2012). First large-scale DNA barcoding assessment of reptiles in the biodiversity hotspot of Madagascar, based on newly designed COI primers. *PLoS One*, *7*, e34506.

Nagy, Z. T., Marion, A. B., Glaw, F., Miralles, A., Nopper, J., Vences, M., & Hedges, S. B. (2015). Molecular systematics and undescribed diversity of Madagascan scolecophidian snakes (Squamata: Serpentes). *Zootaxa*, *4040*, 31–47.

Paris, B. (1999). Espéces de faune et flore connues en RFI des Comores. *Moroni: Projet de Conservation de la biodiversité et Developpement Durable (PNUD/FEM)*, (59). Moroni: Projet de conservation de la biodiversité et développement durable (PNUD/FEM).

Pyron, R., & Wallach, V. (2014). Systematics of the blindsnakes (Serpentes: Scolecophidia: Typhlopoidea) based on molecular and morphological evidence. *Zootaxa*, *3829*, 1–81.

Renoult, J. P., & Raselimanana, A. P. (2009). A new species of Malagasy blind snake of the genus *Typhlops* Oppel (Serpentes: Typhlopidae). *Zootaxa*, *2290*, 65–68.

Rieppel, O., Kley, N. J., & Maisano, J. A. (2009). Morphology of the skull of the white-nosed blindsnake, *Liotyphlops albirostris* (Scolecophidia: Anomalepididae). *Journal of Morphology*, *270*, 536–557.

Ronquist, F., Teslenko, M., van der Mark, P., Ayres, D. L., Darling, A., Höhna, S., … Huelsenbeck, J. P. (2012). MrBayes 3.2: Efficient Bayesian phylogenetic inference and model choice across a large model space. *Systematic Biology*, *61*, 539–542.

Strong, C., Scherz, M. D., & Caldwell, M. W. (n.d.). Deconstructing the gestalt: New concepts and tests of homology, as exemplified by a re-conceptualization of "microstomy" in squamates. *The Anatomical Record*.

Tihen, J. A. (1945). Notes on the osteology of typhlopid snakes. *Copeia*, *4*, 204–210.

Trifinopoulos, J., Nguyen, L. T., von Haeseler, A., & Minh, B. Q. (2016). W-IQ-TREE: A fast online phylogenetic tool for maximum likelihood analysis. *Nucleic Acids Research*, *44*, 232–235.

Wallach, V., & Glaw, F. (2009). A new mid-altitude rainforest species of *Typhlops* (Serpentes: Typhlopidae) from Madagascar with notes on the taxonomic status of *T. boettgeri* Boulenger, *T. microcephalus* Werner, and *T. capensis* Rendahl. *Zootaxa*, *2294*, 23–38.

Wallach, V., Williams, K. L., & Boundy, J. (2014). *Snakes of the world*. Boca Raton: CRC Press.

Warren, B. H., Strasberg, D., Bruggemann, J. H., Prys-Jones, R. P., & Thébaud, C. (2010). Why does the biota of the Madagascar region have such a strong Asiatic flavour? *Cladistics*, *26*, 526–538.

Wegener, J. E., Swoboda, S., Hawlitschek, O., Franzen, M., Wallach, V., Vences, M., … Glaw, F. (2013). Morphological variation and taxonomic reassessment of the endemic Malagasy blind snake family Xenotyphlopidae. *Spixiana*, *36*, 269–282.